A&A 409, 331–345 (2003)
DOI: 10.1051/0004-6361:20031104

Astronomy & Astrophysics

Nonlinear excitation of kinetic Alfvén waves and whistler waves by electron beam-driven Langmuir waves in the solar corona

Yu. Voitenko[1,2], M. Goossens[1], O. Sirenko[1], and A. C.-L. Chian[3,4]

[1] Centre for Plasma Astrophysics, K.U. Leuven, Celestijnenlaan 200B, 3001 Heverlee, Belgium
[2] Main Astronomical Observatory, National Academy of Sciences of Ukraine, 27 Akademika Zabolotnoho St., 03680 Kyiv, Ukraine
[3] National Institute for Space Research – INPE, PO Box 515, 12201-970 Sao Jose dos Campos-SP, Brazil
[4] World Institute for Space Research – WISER, University of Adelaide, SA 5005, Australia

Received 15 May 2003 / Accepted 16 July 2003

Abstract. We study a new nonlinear excitation mechanism of kinetic Alfvén waves (KAWs) and whistler waves (Ws) by electron beam-driven Langmuir waves (Ls). The generation conditions for the parametric decay instability L $\rightleftarrows$ W + KAW are determined and the growth rate is calculated. We show that the resonant pairs of KAWs and whistler waves are nonlinearly coupled to the pump Langmuir waves and their amplitudes undergo exponential growth from the thermal level. The perpendicular dispersion of KAWs strongly increases the coupling due to the nonlinear current parallel to the ambient magnetic field. Our study suggests that the nonlinear coupling of Langmuir wave energy into KAWs and whistlers can provide an efficient sink for weakly dispersive Langmuir waves excited by fast electron beams in the solar corona when the electron plasma frequency is lower than the electron gyrofrequency. This condition can be satisfied in the low-density magnetic filaments that are rooted in the depleted patches at the coronal base and extend to the high corona. At the same time, the Langmuir-driven KAWs and whistlers give rise to scattering and/or thin structures of radio emission penetrating through, or generated in these regions. Since the decay into sunward propagating KAWs is strongest, the nonlinearly driven KAWs can be easily distinguished from the waves generated at the coronal base and propagating away from the Sun. Our results may be used in the analysis of solar radio data and for remote probing of the coronal plasma, magnetic fields, and waves.

Key words. Sun: corona – waves – instabilities

1. Introduction

Nonlinear wave-wave interactions significantly modify the transformation and transport of energy in space plasmas. A wave mode that is excited in an unstable plasma region can be nonlinearly converted into wave modes which posses quite different propagation and dissipation properties. These secondary modes are able to deliver energy and information over long distances and deposit the energy in ways that may be totally different from what is expected for the original wave. Langmuir waves (Ls) are an important example of this type of behavior. They are excited in the solar corona and solar wind by fast electron beams and, in turn, nonlinearly excite radio waves that freely propagate through interplanetary space and are observed on the Earth. This scenario has been first proposed by Ginzburg & Zhelezniakov (1958), and related processes have extensively studied since then (Cairns & Robinson 1998, and references therein).

The nonlinear stabilization of the beam-driven Langmuir instability (Papadopoulos et al. 1974; Grognard 1982; Cairns & Robinson 1998), and/or reabsorption of Langmuir waves by beam (Zaitsev et al. 1972; Mel'nik et al. 1999) can preserve the beam propagation and the Langmuir turbulence can survive over long distances in the solar corona and solar wind. The time-of-flight effects are also important and, together with beam/plasma nonuniformities, can produce stochastically an unstable electron bump-on-tail at any distance from the Sun. On the base of this last consideration, Robinson (1992) introduced a stochastic growth model for Langmuir waves.

The efficiency of these processes depends on the local plasma parameters, and the various possibilities have to be carefully examined when the nonlinear dynamics of Langmuir waves can be determined by alternative processes. So, in their study of the nonlinear dynamics of Langmuir waves, excited by electron beams in the solar corona and solar wind, Cairns & Robinson (1998) argue in favor of the electrostatic decay L $\rightleftarrows$ S + L′ (in its random phase version) rather than the modulational instability,

Send offprint requests to: Yu. Voitenko, e-mail: Yuriy.Voitenko@wis.kuleuven.ac.be

which was first discussed in this context by Papadopoulos et al. (1974), and wave collapse. The nonlinear plasma emission mechanisms involving ion-sound waves (S) are commonly accepted for explaining type III radio emission. The original beam-driven Langmuir waves nonlinearly decay into secondary Langmuir waves plus ion-acoustic waves ($L \rightleftarrows L' + S$), and/or into (fundamental harmonic) radio waves plus ion-acoustic waves ($L \rightleftarrows T_1 + S$), and/or or scatter off thermal ions. In turn, the nonlinear coupling of two Langmuir waves produces the second harmonic radio emission ($L + L' \rightleftarrows T_2$). The coupling of ion-acoustic waves with Langmuir waves ($S + L \rightleftarrows T_1$) provides yet another channel for the fundamental radio emission, but the former, $L \rightleftarrows T_1 + S$, seems to be more favorable (e.g., Thejappa & MacDowall 1998; Bárta & Karlický 2000).

Close temporal correlation between high-frequency Langmuir waves and low-frequency electromagnetic whistler waves has been observed recently within magnetic holes of the solar wind. In order to account for these observations, a theory has been formulated of the nonlinear coupling of Langmuir waves and whistler waves (Chian & Abalde 1999; Luo et al. 1999). It is suggested that the nonlinear interaction of Langmuir waves with whistler waves may lead to the formation of modulated Langmuir wave packets as well as the generation of circularly polarized radio waves at the plasma frequency in the solar wind.

On the other hand, two high-frequency waves with similar frequencies can nonlinearly couple via three-wave resonant interaction with a low-frequency electromagnetic wave. Several nonlinear mode-mode coupling processes, involving high-frequency electrostatic waves and low-frequency Alfvén waves, have been discussed in the past. The nonlinear generation of nonthermal electromagnetic radiation near the electron plasma frequency by Langmuir waves in space and astrophysical plasmas has been studied by Chian et al. (1994, 1997, 2000, 2002) and Lopes & Chian (1996). It was shown that large-amplitude Langmuir waves may explain the excitation of whistler-mode emission in the Earth's and Jupiter's auroral acceleration regions where the electron plasma frequency is smaller than the electron cyclotron frequency. The nonlinear coupling of Langmuir waves with Alfvén waves or whistlers can produce bursty radio emission from flares on the Sun and stars (Chian et al. 1997). All these papers restricted their analysis to interacting waves that propagate along the magnetic field.

The Alfvén waves with high perpendicular wavenumbers are known as kinetic Alfvén waves (KAWs). Linear and nonlinear properties of KAW attract increasing interest because of the strong wave-wave and wave-particle interactions that they cause (Voitenko 1998; Hollweg 1999). Nonlinear parametric processes involving oblique upper-hybrid and oblique (kinetic) Alfvén waves have been investigated by Yukhimuk et al. (1998, 1999). The nonlinear wave-wave couplings are shown to occur due to the electrostatic properties of the oblique Alfvén wave, which greatly increase the efficiency of the coupling processes. In particular, it has been shown that an upper-hybrid wave can parametrically decay into an another upper-hybrid wave and a kinetic Alfvén wave (Yukhimuk et al. 1998). Nonlinear excitation mechanism of high-frequency *x*- and *o*-mode waves by upper hybrid waves has been proposed by Yukhimuk et al. (1999). The parametric decay channels for an upper hybrid wave decaying into high-frequency *x*- and *o*-mode waves and a KAW taking part have been calculated with a special attention towards their possible role in the generation of radio emission from space plasmas. The same oblique Alfvén wave mode, KAW, can interact also with other high-frequency waves, namely – whistlers. A three-wave decay process in which two whistlers and a KAW has been considered by Chen (1977) and Taranenko & Chmyrev (1988). Here the parametric decay involves pump and daughter whistler waves and a daughter KAW. Again, the nonlinear coupling here is possible due to kinetic effects in KAWs.

Obviously, Alfvén waves with short perpendicular wavelengths are important in space plasma, and the extension of the nonlinear analysis of the wave processes including KAWs should reveal more about the fundamental physics involved (Hollweg 1999; Voitenko & Goossens 2000). In present paper we deal with a new nonlinear process in which kinetic Alfvén waves participate: the parametric excitation of KAWs and whistler waves by Langmuir waves. Besides theoretical interest, we study this process in view of its potential importance for the interpretation of the radio observations of complex wave events in the solar corona where Langmuir waves are supposed to be excited by electron beams.

The coherent wave description that we use here is directly applicable to the situation when narrow-band Lanmuir waves are excited by an electron beam. Otherwise, when the bandwidth of Langmuir waves exceeds the calculated nonlinear growth rate, a random-phase analysis should be applied (Cairns & Robinson 1998; Luo et al. 1999). The coupling coefficients that we calculated from the dynamic equation still determine the efficiency of the random-phase decay, but with the growth rate reduced by the wave dephasing. The extension of the coherent analysis of the present paper to the random-phase analysis is thus straightforward but somehaw involved, and is postponed to a separate study. In the Discussion section we provide some numerical estimations of the applicability of the parametric decay approach in corona.

The plasma emission theory based on the Langmuir wave instability has been mainly developed for plasmas with a relatively high density and/or weak magnetic field where the local electron-cyclotron frequency is smaller than the local plasma frequency, $\Omega_e/\omega_{pe} < 1$. This condition is satisfied in the solar wind, and is believed to be satisfied in the solar corona also. However, low values of coronal β (gas/magnetic pressure ratio) allow strong variations of plasma density across the background magnetic field even if the magnetic field varies slowly. Therefore, the magnetic filaments (or threads, or flux tubes), which are rooted in underdense (underheated) patches of the coronal base, should be underdense in the low-β coronal plasma as well, and the condition $\Omega_e/\omega_{pe} > 1$ can be satisfied. The electron beam-driven Langmuir instability is still strong in this situation (e.g., Vlahos & Rowland 1984), but the nonlinear processes involved can be quite different. In particular, our present study suggests that the Alfvén-whistler turbulence may provide an efficient energy sink for Langmuir waves in a diluted solar plasma where the electron-cyclotron frequency is larger than the plasma frequency, $\Omega_e/\omega_{pe} \gtrsim 1$.

2. Basic equations and plasma model

We consider an oblique Langmuir wave with

$$\boldsymbol{E}_{\rm L} = (E_{{\rm L}x}\boldsymbol{e}_x + E_{{\rm L}z}\boldsymbol{e}_z)\exp\left[-i\left(\omega_{\rm L}t - k_{{\rm L}x}x - k_{{\rm L}z}z\right)\right] + \text{c.c};$$

$$k_{{\rm L}z} > 0,$$

propagating in an homogeneously magnetized plasma ($B_0 = B_0 e_z$). As the solar corona is nonuniform, the approximation of a uniform plasma means here that the parallel and perpendicular length scales of the plasma inhomogeneities are much longer than the respective wavelengths which appear in the problem: $L_z \gg \lambda_z = 2\pi/k_z$; $L_x \gg \lambda_x = 2\pi/k_x$.

An important parameter is the electron cyclotron/electron plasma frequency ratio $\Omega_{\rm e}/\omega_{\rm pe}$. In the solar wind $\Omega_{\rm e}/\omega_{\rm pe} \ll 1$, as is measured in situ by satellites, and it is widely believed that at least $\Omega_{\rm e}/\omega_{\rm pe} < 1$ in the coronal type III bursts. Here we note that the coronal heating process is highly non-uniform, which causes large cross-field density variations of the plasma evaporated from the chromosphere. As the strong magnetic field (MF) confines the plasma across MF lines in a low-β coronal plasma, the hydrostatic equilibrium along MF lines gives rise to a very nonuniform plasma density across MF in the high corona also. Namely, the particle density decreases faster with height where the temperature is lower, i.e., where the plasma is underheated. In this situation, significant variations of the plasma density can appear across the MF (i.e., in the horizontal direction). The force balance in that direction involves both the gas pressure and the magnetic pressure forces. Since the magnetic field lines are frozen in the plasma, the perpendicular imbalance of gas pressure produces the (small in low-β plasma) variations of the magnetic pressure that keep the total pressure constant in the horizontal direction. The cross-field non-uniformities are observed in the form of filamentary ray-like structures, extending radially from the coronal base in the corona (Woo 1996). The perpendicular length scales of density filaments are as small as 1 km at the coronal base, and about 10 km at 2–5 solar radii. Hence we adopt the opposite inequality, $\Omega_{\rm e}/\omega_{\rm pe} > 1$, for low-density magnetic filaments magnetically connected with the cool patches at the coronal base.

We are interested in the temporal evolution of a trial whistler wave with frequency $\omega_{\rm W}$ and wave vector $\boldsymbol{k}_{\rm W} = \{0; 0; k_{{\rm W}z}\}$ and a kinetic Alfvén wave (KAW) with frequency $\omega_{\rm A}$ and wave vector $\boldsymbol{k}_{\rm A} = \{k_{{\rm A}x}; 0; k_{{\rm A}z}\}$ with $k_{{\rm A}x} >> k_{{\rm A}z}$. The whistler wave and the kinetic Alfvén wave are coupled via a pump Langmuir wave with frequency $\omega_{\rm L}$ and wave vector $\boldsymbol{k}_{\rm L} = \{k_{{\rm L}x}; 0; k_{{\rm L}z}\}$. For a strong three-wave coupling, the following resonant conditions should be satisfied:

$$\omega_{\rm L} = \omega_{\rm W} + \omega_{\rm A}; \tag{1}$$

$$k_{{\rm L}x} = k_{{\rm A}x}; \quad k_{{\rm L}z} = k_{{\rm W}z} + k_{{\rm A}z}. \tag{2}$$

We choose $k_{{\rm L}z} > 0$. Then $k_{{\rm A}z}$ can be >0 (for parallel-propagating KAW) or <0 (for antiparallel-propagating KAW), but $k_{{\rm W}z}$ is always >0 because $|k_{{\rm A}z}| < k_{{\rm L}z}$.

The KAWs are low-frequency waves, $\omega_{\rm A} < \Omega_{\rm p}$ ($\Omega_{\rm p}$ is the proton cyclotron frequency), and the Langmuir waves are high-frequency waves, with frequencies of the order of electron plasma frequency, $\omega_{\rm L} \approx \omega_{\rm pe} \gg \Omega_{\rm p}$. Hence, the resonant condition (1) can be satisfied if $\omega_{\rm W} \approx \omega_{\rm L}$. Having in mind that the whistler frequency $\omega_{\rm W} < \Omega_{\rm e}$, we see that the resonant condition can be easily satisfied only when $\omega_{\rm pe} < \Omega_{\rm e}$, as we choose in our plasma model (see Sect. 4.1 for more quantitative discussion of resonant conditions).

The wave electromagnetic fields obey Maxwell's equations

$$\boldsymbol{\nabla} \times \boldsymbol{B} = \frac{4\pi}{c}\boldsymbol{j} + \frac{1}{c}\frac{\partial \boldsymbol{E}}{\partial t}, \tag{3}$$

$$\boldsymbol{\nabla} \times \boldsymbol{E} = -\frac{1}{c}\frac{\partial \boldsymbol{B}}{\partial t}, \tag{4}$$

$$\boldsymbol{\nabla} \cdot \boldsymbol{E} = 4\pi Q, \tag{5}$$

where the current density, $\boldsymbol{j} = \sum_{\rm s} q_{\rm s} n_{\rm s} \boldsymbol{v}_{\rm s}$, and the charge density, $Q = \sum_{\rm s} q_{\rm s} n_{\rm s}$, have to be calculated using a suitable mathematical model of the plasma. The most popular models are based on the ideal MHD equations, the two-fluid MHD equations, and the kinetic Vlasov equations. We use the mathematical model of two-fluid MHD that permits us to take into account both the high-frequency electronic waves (Langmuir and whistlers), and important linear and nonlinear effects that arise in short-scale (kinetic) Alfvén waves. Therefore, all the interacting waves are described with the model equations of warm two-fluid MHD:

$$\frac{\partial \boldsymbol{V}_{\rm s}}{\partial t} = \frac{q_{\rm s}}{m_{\rm s}}\left(\boldsymbol{E} + \frac{1}{c}\boldsymbol{V}_{\rm s} \times \boldsymbol{B}_0\right) - \frac{T_{\rm s}}{n_{\rm s} m_{\rm s}}\boldsymbol{\nabla} n_{\rm s} + \frac{1}{m_{\rm s}}\boldsymbol{F}_{\rm s}, \tag{6}$$

$$\frac{\partial n_{\rm s}}{\partial t} = -\boldsymbol{\nabla}(n_{\rm s}\boldsymbol{V}_{\rm s}), \tag{7}$$

where

$$\boldsymbol{F}_\mathrm{s} = \frac{e_\mathrm{s}}{c}(\boldsymbol{V}_\mathrm{s} \times \boldsymbol{B}) - m_\mathrm{s}(\boldsymbol{V}_\mathrm{s} \cdot \boldsymbol{\nabla})\boldsymbol{V}_\mathrm{s}.$$

The index s = p, e corresponds to the protons and electrons respectively. The electron density and velocity, the electric and magnetic fields are presented in the form:

$$n_\mathrm{e} = n_0 + n_\mathrm{eL} + n_\mathrm{eA}; \tag{8}$$

$$\boldsymbol{V}_\mathrm{e} = \boldsymbol{V}_\mathrm{eL} + \boldsymbol{V}_\mathrm{eW} + \boldsymbol{V}_\mathrm{eA};$$

$$\boldsymbol{E} = \boldsymbol{E}_\mathrm{L} + \boldsymbol{E}_\mathrm{W} + \boldsymbol{E}_\mathrm{A};$$

$$\boldsymbol{B} = \boldsymbol{B}_\mathrm{A} + \boldsymbol{B}_\mathrm{W}.$$

$$\boldsymbol{B}_0 = \boldsymbol{e}_z B_0.$$

Here n_0 and B_0 are the average values of the plasma number density and magnetic field. The subscripts L, W, and A in these expressions correspond to the perturbations due to Langmuir, whistler and KAW respectively.

2.1. Nonlinear dispersion relation for KAWs

The plasma/magnetic pressure ratio β plays an important role for KAWs. Indeed, the electron and/or proton temperature effects prevail when $m_\mathrm{e}/m_\mathrm{p} < \beta < 1$, while the parallel electron inertia effects are more important for $\beta < m_\mathrm{e}/m_\mathrm{p}$. Although the condition $m_\mathrm{e}/m_\mathrm{p} < \beta < 1$ holds for most of the solar corona, there are regions of diluted cold plasma and/or strong magnetic field, e.g., above magnetic spots, where $\beta < m_\mathrm{e}/m_\mathrm{p}$. Therefore, we take into account both the temperature effects, and the parallel electron inertia effects for KAWs.

Since KAWs are low-frequency waves, the plasma approximation (quasi-neutrality condition) holds:

$$n_\mathrm{eA} = n_\mathrm{pA}. \tag{9}$$

We calculate the expressions for the electron and proton number densities related to the KAW, n_eA and n_pA, from the equations of motion (6) and the continuity Eqs. (7). Thus we find

$$\frac{n_\mathrm{eA}}{n_0} = \frac{e}{T_\mathrm{e}}\frac{1}{1 - V_{k\mathrm{A}}^2/V_{T\mathrm{e}}^2}(\varphi - A) + \frac{e}{T_\mathrm{e}}\frac{1}{1 - V_{k\mathrm{A}}^2/V_{T\mathrm{e}}^2}\left[\frac{F_{ez}}{iek_{\mathrm{A}z}} - \frac{T_\mathrm{e}}{e}\frac{V_{k\mathrm{A}}^2}{V_{T\mathrm{e}}^2}\left(\frac{n}{n_0}\right)_\mathrm{e}^{NL} - \frac{m_\mathrm{e}}{m_\mathrm{p}}\mu_\mathrm{s}\frac{V_{k\mathrm{A}}^2}{V_{T\mathrm{e}}^2}\frac{1}{iek_{\mathrm{A}x}}\left(F_{ex} - \frac{i\Omega_\mathrm{e}}{\omega_\mathrm{A}}F_{ey}\right)\right]; \tag{10}$$

$$\frac{n_\mathrm{pA}}{n_0} = -\frac{e}{T_\mathrm{p}}\frac{\mu_\mathrm{p}}{1 + \mu_\mathrm{p}}\left[\varphi + \frac{1}{\mu_\mathrm{p}}\frac{V_{T\mathrm{p}}^2}{V_{k\mathrm{A}}^2}A\right], \tag{11}$$

where μ_p and μ_s are dispersion variables $\mu_\mathrm{p} = k_{\mathrm{A}x}^2\rho_\mathrm{p}^2$, $\mu_\mathrm{s} = \mu_\mathrm{p}T_\mathrm{e}/T_\mathrm{p}$, ρ_p is the proton gyroradius $\rho_\mathrm{p} = V_{T\mathrm{p}}/\Omega_\mathrm{p}$, $V_{T\mathrm{p}} = \sqrt{T_\mathrm{p}/m_\mathrm{p}}$ is the proton thermal velocity, $V_{k\mathrm{A}} = \omega_\mathrm{A}/k_{\mathrm{A}z}$ is the wave phase speed, $A = (\omega_\mathrm{A}/k_{\mathrm{A}z}c)A_z$, φ and A_z are the scalar and vector electromagnetic potentials due to KAWs, and

$$\left(\frac{n}{n_0}\right)_\mathrm{e}^{NL} = \frac{\boldsymbol{k}_\mathrm{A}}{\omega_\mathrm{A}}\left(\frac{n_\mathrm{e}}{n_0}\boldsymbol{V}_\mathrm{e}\right)_{NL}.$$

This last nonlinearity originates from the divergence of the nonlinear particles flux $n_\mathrm{e}\boldsymbol{V}_\mathrm{e}$ in the electron continuity Eq. (7) with s = e.

When we take into account that the electric current along the magnetic field for a plasma with $\beta \ll 1$ is determined mostly by electrons, we obtain from the parallel component of Ampere law (3) that

$$\frac{n_\mathrm{eA}}{n_0} = \frac{e}{T_\mathrm{e}}\left[\varphi - \left(1 + k_\mathrm{A}^2\delta_\mathrm{e}^2\right)A + \frac{F_{ez}}{iek_{\mathrm{A}z}} - \frac{m_\mathrm{e}}{e}\frac{\omega_\mathrm{A}}{k_{\mathrm{A}z}}\frac{n_\mathrm{e}^L}{n_0}V_{\mathrm{e}z}^L\right], \tag{12}$$

where $\delta_\mathrm{e} = c/\omega_\mathrm{pe}$ is the electron inertial length.

The nonlinear second-order dispersion relation is found from Eqs. (9)–(12):

$$D_\mathrm{A}E_{\mathrm{A}x} = N_\mathrm{A}. \tag{13}$$

D_A denotes the linear dispersion and is given by

$$D_\mathrm{A} = \omega_\mathrm{A}^2 - k_{\mathrm{A}z}^2V_\mathrm{A}^2K^2,$$

where the dispersion function for the KAW K determines the wave phase velocity:

$$\frac{\omega_{\rm A}}{k_{\rm Az}V_{\rm A}} \equiv K = \sqrt{\frac{1+\mu_T}{1+\chi_{\rm e}}}, \tag{14}$$

and the dispersive variables for KAW are $\mu_T = \mu_{\rm p} + \mu_{\rm s}$ and $\chi_{\rm e} = k_{{\rm A}x}^2\delta_{\rm e}^2$.

The nonlinear part $N_{\rm A}$ is given by

$$N_{\rm A} = k_{\rm Az}^2 V_{\rm A}^2 \frac{1+\mu_{\rm p}}{1+\chi_{\rm e}} \left\{ \frac{m_{\rm e}}{e} i\omega_{\rm A} \frac{k_{{\rm A}x}}{k_{\rm Az}} \left[\left(\frac{n_{\rm e}^L}{n_0} V_{{\rm e}z}^L \right) + \frac{1+\chi_{\rm e}}{\chi_{\rm e}} \frac{k_{{\rm A}x}}{k_{\rm Az}} \left(\frac{n_{\rm e}^L}{n_0} V_{{\rm e}x}^L \right) \right] + \frac{m_{\rm e}}{m_{\rm p}} \frac{V_{k{\rm A}}^2}{V_{\rm A}^2} (1+\chi_{\rm e}) \frac{1}{e} \left(F_{{\rm e}x} - i\frac{\Omega_{\rm e}}{\omega_{\rm A}} F_{{\rm e}y} \right) - \frac{1}{e} \frac{k_{{\rm A}x}}{k_{\rm Az}} F_{{\rm e}z} \right\}. \tag{15}$$

2.2. Nonlinear dispersion relation for the whistler

For high-frequency whistlers we can neglect the proton dynamics. With this assumption the Maxwell equations for parallel-propagating whistler wave, $k_{\rm W} = (0; 0; k_{\rm W})$, give

$$\begin{aligned} \left(\omega^2 - c^2k_{\rm W}^2\right) E_{{\rm W}x} &= 4\pi i\omega e n_{\rm W} V_{{\rm W}x}, \\ \left(\omega^2 - c^2k_{\rm W}^2\right) E_{{\rm W}y} &= 4\pi i\omega e n_{\rm W} V_{{\rm W}y}, \end{aligned} \tag{16}$$

where we have dropped the subindex "e" that denotes the electron species.

From the equation of motion (6) we obtain the electron velocity components due to whistler:

$$\begin{aligned} V_{{\rm W}x} &= \frac{e}{m_{\rm e}\omega_{\rm W}} \left(-iE_{{\rm W}x} - \frac{\Omega_{\rm e}}{\omega_{\rm W}} E_{{\rm W}y} \right) \left(1 - \frac{\Omega_{\rm e}^2}{\omega_{\rm W}^2} \right)^{-1} + \frac{1}{m_{\rm e}\omega_{\rm W}} \left(iF_{{\rm W}x} + \frac{\Omega_{\rm e}}{\omega_{\rm W}} F_{{\rm W}y} \right); \\ V_{{\rm W}y} &= \frac{e}{m_{\rm e}\omega_{\rm W}} \left(-iE_{{\rm W}y} + \frac{\Omega_{\rm e}}{\omega_{\rm W}} E_{{\rm W}x} \right) \left(1 - \frac{\Omega_{\rm e}^2}{\omega_{\rm W}^2} \right)^{-1} + \frac{1}{m_{\rm e}\omega_{\rm W}} \left(iF_{{\rm W}y} - \frac{\Omega_{\rm e}}{\omega_{\rm W}} F_{{\rm W}x} \right). \end{aligned}$$

Then using these electron velocities in the Maxwell Eqs. (16), we find the second-order dispersion relation for whistlers:

$$D_{\rm W} E_{{\rm W}x} = N_{\rm W}. \tag{17}$$

Here the dispersive term is

$$D_{\rm W} = \omega_{\rm W}^2 - c^2k_{{\rm W}z}^2 - \omega_{\rm pe}^2 \frac{\omega_{\rm W}}{(\omega_{\rm W} - \Omega_{\rm e})},$$

and the nonlinear term is

$$N_{\rm W} = \frac{1}{2e}\omega_{\rm pe}^2 \left(1 + \frac{\Omega_{\rm e}}{\omega_{\rm W}} \right) \left(iF_{{\rm W}y} - F_{{\rm W}x} \right) + 2\pi e\omega_{\rm W} n (V_y + iV_x). \tag{18}$$

3. Plasma response

In order to calculate the nonlinear coupling coefficients we need explicit expressions for the linear responses due to all wave modes, i.e. linear expressions for the electron velocity components, electron density perturbations and magnetic field perturbations.

3.1. Linear response due to Langmuir wave

In the Langmuir wave,

$$\frac{n_{\rm eL}}{n_0} = -\frac{e}{m_{\rm e}} \frac{k_{\rm L}^2}{\omega_{\rm pe}^2} \varphi_{\rm L}; \tag{19}$$

$$V_{{\rm L}x} = -\frac{e}{m_{\rm e}} \frac{k_{{\rm L}x}}{\omega_{\rm L}} \left(1 + V_{{\rm T}e}^2 \frac{k_{\rm L}^2}{\omega_{\rm pe}^2} \right) \left(1 - \frac{\Omega_{\rm e}^2}{\omega_{\rm L}^2} \right)^{-1} \varphi_{\rm L}; \tag{20}$$

$$V_{{\rm L}y} = i\frac{e}{m_{\rm e}} \frac{k_{{\rm L}x}}{\omega_{\rm L}} \frac{\Omega_{\rm e}}{\omega_{\rm L}} \left(1 + V_{{\rm T}e}^2 \frac{k_{\rm L}^2}{\omega_{\rm pe}^2} \right) \left(1 - \frac{\Omega_{\rm e}^2}{\omega_{\rm L}^2} \right)^{-1} \varphi_{\rm L}; \tag{21}$$

$$V_{\mathrm{L}z} = -\frac{e}{m_\mathrm{e}}\frac{k_{\mathrm{L}z}}{\omega_\mathrm{L}}\left(1 + V_{T\mathrm{e}}^2\frac{k_\mathrm{L}^2}{\omega_\mathrm{pe}^2}\right)\varphi_\mathrm{L}. \tag{22}$$

The dispersion equation is found from Poisson's law and the continuity equation:

$$\frac{\omega_\mathrm{L}^2}{\omega_\mathrm{pe}^2}\frac{\omega_\mathrm{L}^2}{\omega_\mathrm{pe}^2} - \left(1 + V_{T\mathrm{e}}^2\frac{k_\mathrm{L}^2}{\omega_\mathrm{pe}^2} + \frac{\Omega_\mathrm{e}^2}{\omega_\mathrm{pe}^2}\right)\frac{\omega_\mathrm{L}^2}{\omega_\mathrm{pe}^2} = -\frac{k_{\mathrm{L}z}^2}{k_\mathrm{L}^2}\left(1 + V_{T\mathrm{e}}^2\frac{k_\mathrm{L}^2}{\omega_\mathrm{pe}^2}\right)\frac{\Omega_\mathrm{e}^2}{\omega_\mathrm{pe}^2}.$$

The solution for this equation is

$$\omega_\mathrm{L} = \omega_\mathrm{pe} z, \tag{23}$$

where

$$2z^2 = \left(1 + V_{T\mathrm{e}}^2\frac{k_\mathrm{L}^2}{\omega_\mathrm{pe}^2} + \frac{\Omega_\mathrm{e}^2}{\omega_\mathrm{pe}^2}\right) \pm \sqrt{\left(1 + V_{T\mathrm{e}}^2\frac{k_\mathrm{L}^2}{\omega_\mathrm{pe}^2} + \frac{\Omega_\mathrm{e}^2}{\omega_\mathrm{pe}^2}\right)^2 - 4\frac{k_{\mathrm{L}z}^2}{k_\mathrm{L}^2}\left(1 + V_{T\mathrm{e}}^2\frac{k_\mathrm{L}^2}{\omega_\mathrm{pe}^2}\right)\frac{\Omega_\mathrm{e}^2}{\omega_\mathrm{pe}^2}},$$

or, using $k_{\mathrm{L}z}^2 = k_\mathrm{L}^2 - k_{\mathrm{L}x}^2$,

$$z^2 = \frac{1}{2}\left[\left(1 + Y^2 + b^2\right) \pm \sqrt{\left(1 + Y^2 - b^2\right)^2 + 4\frac{X^2}{Y^2}\left(1 + Y^2\right)b^2}\right], \tag{24}$$

where the normalized wavenumbers $Z = k_{\mathrm{L}z}\lambda_\mathrm{D}$, $X = k_{\mathrm{L}x}\lambda_\mathrm{D}$, $Y = \sqrt{X^2 + Z^2} = k_\mathrm{L}\lambda_\mathrm{D}$, $\lambda_\mathrm{D} = V_{T\mathrm{e}}/\omega_\mathrm{pe}$ is the electron Debye length. The quantity $b = \Omega_\mathrm{e}/\omega_\mathrm{pe}$ (electron cyclotron/electron plasma frequency ratio) will play an important role in what follows. For Langmuir branch in the range $1 + Y^2 - b^2 < 0$, we take "–" in (24).

When the first term dominate under the square root in (24) (e.g., for quasi-parallel waves $k_{\mathrm{L}x}^2 \ll k_\mathrm{L}^2$),

$$z^2 = \frac{1}{2}\left(1 + Y^2 + b^2\right) \pm \frac{1}{2}\left[\left|1 + Y^2 - b^2\right| + 2\frac{X^2}{Y^2}\left(1 + Y^2\right)b^2\left|1 + Y^2 - b^2\right|^{-1}\right].$$

Taking $+\,(-)$ for $1 + Y^2 - b^2 > (<)\,0$, we get

$$z^2 = \left(1 + Y^2\right)\left(1 + \frac{X^2}{Y^2}\frac{b_{T\mathrm{e}}^2}{1 - b_{T\mathrm{e}}^2}\right),$$

where

$$b_{T\mathrm{e}}^2 = b^2\left(1 + Y^2\right)^{-1}.$$

For weak wave dispersion, $Y^2 = k_\mathrm{L}^2\lambda_\mathrm{D}^2 \ll 1$, we have

$$z = \sqrt{1 + Y^2 + \frac{X^2}{Y^2}\frac{b^2}{1 + Y^2 - b^2}}.$$

3.2. Linear response due to whistler

In the whistler wave we have $n_{\mathrm{e}\mathrm{W}} = 0$, and

$$B_{\mathrm{W}x} = -i\frac{c}{\omega_\mathrm{W}}k_\mathrm{W}E_{\mathrm{W}x}; \tag{25}$$

$$B_{\mathrm{W}y} = \frac{c}{\omega_\mathrm{W}}k_\mathrm{W}E_{\mathrm{W}x}; \tag{26}$$

$$V_{\mathrm{W}x} = -i\frac{e}{m_\mathrm{e}\omega_\mathrm{W}}\left(1 - \frac{\Omega_\mathrm{e}}{\omega_\mathrm{W}}\right)^{-1}E_{\mathrm{W}x}; \tag{27}$$

$$V_{\mathrm{W}y} = \frac{e}{m_\mathrm{e}\omega_\mathrm{W}}\left(1 - \frac{\Omega_\mathrm{e}}{\omega_\mathrm{W}}\right)^{-1}E_{\mathrm{W}x}. \tag{28}$$

The dispersion is

$$\frac{\omega_\mathrm{W}^2}{\omega_\mathrm{pe}^2} = c^2\frac{k_{\mathrm{W}z}^2}{\omega_\mathrm{pe}^2} + \frac{\omega_\mathrm{W}}{(\omega_\mathrm{W} - \Omega_\mathrm{e})}. \tag{29}$$

3.3. Linear response due to kinetic Alfvén wave

In the kinetic Alfvén wave

$$\frac{n_{\rm Ae}}{n_0} = -i\frac{e}{m_{\rm e}}\frac{1}{V_{Te}^2 k_{{\rm A}x}}\frac{\mu_{\rm s}}{1+\mu_{\rm p}}E_{{\rm A}x}; \tag{30}$$

$$V_{{\rm A}x} = i\frac{e}{m_{\rm e}}\frac{\omega_{\rm A}}{\Omega_{\rm e}^2}E_{{\rm A}x}\left[1-\frac{m_{\rm p}}{m_{\rm e}}\beta\frac{1}{1+\mu_{\rm p}}+\frac{\mu_{\rm s}}{1+\mu_{\rm p}}\right]; \tag{31}$$

$$V_{{\rm A}y} = -\frac{e}{m_{\rm e}}\frac{1}{\Omega_{\rm e}}\left[1+\frac{\mu_{\rm s}}{1+\mu_{\rm p}}\right]E_{{\rm A}x}; \tag{32}$$

$$V_{{\rm A}z} = -i\frac{e}{m_{\rm e}}\frac{k_{{\rm A}x}}{k_{\rm Az}}\frac{\omega_{\rm A}}{\Omega_{\rm e}^2}\frac{m_{\rm p}}{m_{\rm e}}\frac{1}{1+\mu_{\rm p}}E_{{\rm A}x}; \tag{33}$$

$$B_{{\rm A}y} = \frac{ck_{\rm Az}}{\omega_{\rm A}}\left[1+\frac{\mu_{\rm s}}{1+\mu_{\rm p}}\left(1-\frac{V_{kA}^2}{V_{Te}^2}\right)\right]E_{{\rm A}x}; \tag{34}$$

$$B_{\rm Az} = -i\frac{ck_{{\rm A}x}}{\Omega_i}\beta\frac{1}{1+\mu_{\rm p}}E_{{\rm A}x}. \tag{35}$$

3.4. Nonlinear response at whistler's spatio-temporal scales

Having found the expressions for the linear plasma response we are now in a position to calculate the second-order nonlinear source part $N_{\rm W} = \varphi_{\rm L}E_{\rm Ax}^*\bar{N}_{\rm W}$ in the equations for whistlers. The calculation is straightforward but somehow involved. Inserting the linear expressions (19)–(22) for the pump Langmuir wave into (18), and (30)–(35) for the trial KAW, and keeping dominant terms, we find the expression for $\bar{N}_{\rm W}$:

$$\bar{N}_{\rm W} = -\frac{1}{2}\omega_{\rm pe}^2\frac{e}{m_{\rm e}}\frac{1}{V_{Te}^2}\frac{m_{\rm p}}{m_{\rm e}}\frac{1}{b^2}\frac{z}{b-z}\frac{1+Y^2}{1+\mu_{\rm p}}\left(X^2 - s_{\rm A}\frac{m_{\rm e}}{m_i}b^3\frac{V_{Te}}{V_{\rm A}}\frac{b^2-z^2}{z^3}KZ\right). \tag{36}$$

Here $s_{\rm A} = k_{\rm Az}/|k_{\rm Az}|$ accounts for the propagation direction of the KAW: $s_{\rm A} = 1$ for forward propagation (i.e., in the direction of the ambient magnetic field), $s_{\rm A} = -1$ for backward (antiparallel) propagation.

3.5. Nonlinear response at KAW's spatio-temporal scales

Similarly, we find the nonlinear source term for KAWs $N_{\rm A}^* = \varphi_{\rm L}^* E_{{\rm W}x}\bar{N}_{\rm A}^*$, where

$$\begin{aligned}\bar{N}_{\rm A}^* = {} & \frac{e}{m_{\rm e}}k_{\rm Az}^2V_{\rm A}^2\frac{1+\mu_{\rm p}}{1+\chi_{\rm e}}\frac{k_{\rm Lz}}{\omega_{\rm L}}\frac{k_{\rm Wz}}{\omega_{\rm W}}\left(1+\frac{k^2V_{Te}^2}{\omega_{\rm pe}^2}\right)\frac{\omega_{\rm Be}}{\omega_{\rm Be}-\omega_{\rm W}}\left\{-\frac{m_{\rm e}}{m_{\rm p}}K^2(1+\chi_{\rm e})\left[1+\frac{k_{{\rm L}x}}{k_{\rm Wz}}\frac{k_{{\rm L}x}}{k_{\rm Lz}}\frac{\omega_{\rm W}}{\omega_{\rm Be}}\frac{\omega_{\rm L}^2}{\omega_{\rm Be}^2-\omega_{\rm L}^2}-\frac{\omega_{\rm Be}}{\omega_{\rm A}}\right.\right.\\ & \left.\left.\times\left(1-\frac{k_{\rm L}^2}{k_{\rm Wz}k_{\rm Lz}}\frac{\omega_{\rm L}\omega_{\rm W}}{\omega_{\rm pe}^2}\left(1+\frac{k_{\rm L}^2V_{Te}^2}{\omega_{\rm pe}^2}\right)^{-1}-\frac{k_{{\rm L}x}}{k_{\rm Wz}}\frac{k_{{\rm L}x}}{k_{\rm Lz}}\frac{\omega_{\rm L}\omega_{\rm W}}{\omega_{\rm Be}^2-\omega_{\rm L}^2}\right)\right]+\frac{k_{{\rm A}x}}{k_{\rm Az}}\frac{k_{{\rm L}x}}{k_{\rm Lz}}\frac{\omega_{\rm W}}{\omega_{\rm Be}-\omega_{\rm L}}\left(\frac{\omega_{\rm A}}{\omega_{\rm W}}+\frac{k_{\rm Az}}{k_{\rm W}}\left(\frac{\omega_{\rm L}}{\omega_{\rm Be}}-1\right)\right)\right\}.\end{aligned} \tag{37}$$

When we simplify this expression by use of the resonant conditions and the dispersion relations for the interacting waves, and keeping dominant terms, we obtain

$$N_{\rm A}^* = -\frac{e}{m_{\rm e}}\frac{k_{\rm L}^2}{\omega_{\rm pe}^2}\frac{b\left(1+\mu_{\rm p}\right)}{b-z}\frac{\omega_{\rm A}\Omega_{\rm p}}{z^2}\frac{X^2}{Y^2}\left(\frac{z}{b\left(1+\mu_T\right)}\frac{\omega_{\rm A}}{\Omega_{\rm p}}-Y^2\right). \tag{38}$$

4. Parametric decay instability $L \rightleftarrows W + KAW$

In this section we investigate the decay of an oblique Langmuir wave into pairs composed of resonant whistlers and KAWs. The proximity of the whistler and Langmuir wave frequencies imposes additional restrictions on this process, therefore we start with an analysis of the resonant conditions.

4.1. Selectivity of the decay

The resonant conditions impose restrictions on the parameters of the interacting waves. We use the frequency matching condition, $\omega_{\rm W} = \omega_{\rm L} - \omega_{\rm A}$, and insert (23) into (29) to get the matching equation relating the parameters of the interacting waves:

$$\left[(z-\nu_{\rm A})^2 - 1 - \frac{1}{\alpha_{Te}^2}\left(Z - s_{\rm A}\frac{V_{Te}}{V_{\rm A}K}\nu_{\rm A}\right)^2\right](z-\nu_{\rm A}-b) - b = 0, \tag{39}$$

where $s_{\rm A} = \boldsymbol{k}_{\rm Az}/|\boldsymbol{k}_{\rm Az}|$ ($s_{\rm A} = \pm 1$), and

$$\alpha_{Te}^2 = \frac{V_{Te}^2}{c^2}; \quad \nu_{\rm A} = \frac{\omega_{\rm A}}{\omega_{\rm pe}}.$$

For any given $Z \ll 1$, the compatibility of the dispersion relation (24) with the resonant condition (39) restricts the possible perpendicular wavenumber X and Alfvén frequency $\nu_{\rm A}$. We use the fact that $\nu_{\rm A}$, α_{Te}^2 are small, and we assume that μ_T is also small. Then, in the case of weak Langmuir dispersion, from Eq. (39) we find an approximate expression for wavenumber X of an unstable Langmuir wave as function of Z and $\nu_{\rm A}$:

$$X = Z\sqrt{\left(1 + 2\frac{b^2-1}{b}\left(\frac{b-1}{b} - \frac{\alpha_{Te}^2}{\left(Z - s_{\rm A}\frac{V_{Te}}{V_{\rm A}K}\nu_{\rm A}\right)^2}\right)\right)^{-1} - 1}. \tag{40}$$

This solution is a good approximation in the range $Z = 0.01$–0.1. This case is physically realizable with Langmuir waves of weak dispersion as long as $1 < b^2 < 2$. For a given values of Z and X, the excited Alfvén waves have frequencies determined by (39).

One should note that the variation of the KAW frequency in the range $0 < \omega_{\rm A} < \Omega_i$ at fixed b produces small deviations of the resonant value of X around the value determined mainly by Z and by plasma parameters, b and α_{Te}. In other words, the matching equation indicates that the decay is possible if the initial Langmuir waves adjust their perpendicular wavenumber X, and/or parallel wavenumber Z, to the value(s) given by the solution of matching Eq. (39). However, the analytical solution (40) is invalid in the range $Z < 0.01$. The resonant diagram, valid for all Z, is shown in Fig. 1.

The resonant perpendicular wavenumber $k_{\rm Lx}^{\rm res}$, given by (39), determines the resonant propagation angle for the Langmuir decay, $\theta_{\rm res} = \arctan k_{\rm Lx}^{\rm res}/k_{\rm Lz}$. If the value of b is sufficiently close to 1 (e.g., $b = 1.02$), the Langmuir waves which develop resonant values of X can decay over a wide range of Z. However, for larger values of b, the allowed range of Z, $Z < Z_1$, shrinks towards low Langmuir wavenumbers with an upper boundary

$$Z_1 \approx \frac{V_{Te}}{c}\sqrt{\frac{b}{b-1}}. \tag{41}$$

Fast electron beams can excite directly such Langmuir waves. For example, $Z_1 \approx 0.047$ for $b = 1.1$ and $V_{Te}/c = 1/70$.

There is another, well separated range of larger resonant Z required for the decay, $Z > Z_2$, with

$$Z_2 \approx \sqrt{b^2-1}. \tag{42}$$

For example, $Z_2 \approx 0.46 \gg Z_1 \approx 0.047$ for $b = 1.1$. The above approximate formulae for Z_1 and Z_2 follow from (39) with $X = 0$. We do not show the $Z > Z_2$ resonant region in Figs. 1 and 2 because the nonlinear growth rate is imaginary for all $Z > Z_1$.

The parallel wavenumbers of the Langmuir waves that are directly excited by slow beams can be in the range $Z > Z_1$ where decay is impossible. In this case there is still a possibility that the waves propagating in the higher-density region will reduce their wavenumbers to $Z \lesssim Z_1$, and eventually meet the resonant condition for decay into KAWs and whistlers. Or some other nonlinear process(es) redistribute Langmuir spectrum towards smaller Z satisfying $Z \lesssim Z_1$.

4.2. Nonlinear growth rate

From (13) and (17), we obtain the nonlinear dispersion relation for the parametric decay instability of Langmuir wave:

$$D_{\rm W}D_{\rm A}^* = \bar{N}_{\rm W}\bar{N}_{\rm A}^*\,|\varphi_{\rm L}|^2\,. \tag{43}$$

When we allow for a dissipative part in the wave frequencies, $\omega_{\rm A,W} = \omega_{\rm A,W} + i\gamma_{NL}$, in (43) we obtain the expression for the nonlinear growth rate γ_{NL}^2:

$$\gamma_{NL}^2 = \frac{b\,(z-b)^2\,\bar{N}_{\rm W}\bar{N}_{\rm A}^*\,|\varphi_{\rm L}|^2}{2\omega_{\rm A}\Omega_{\rm e}\left(2z\,(z-b)^2 + b\right)}. \tag{44}$$

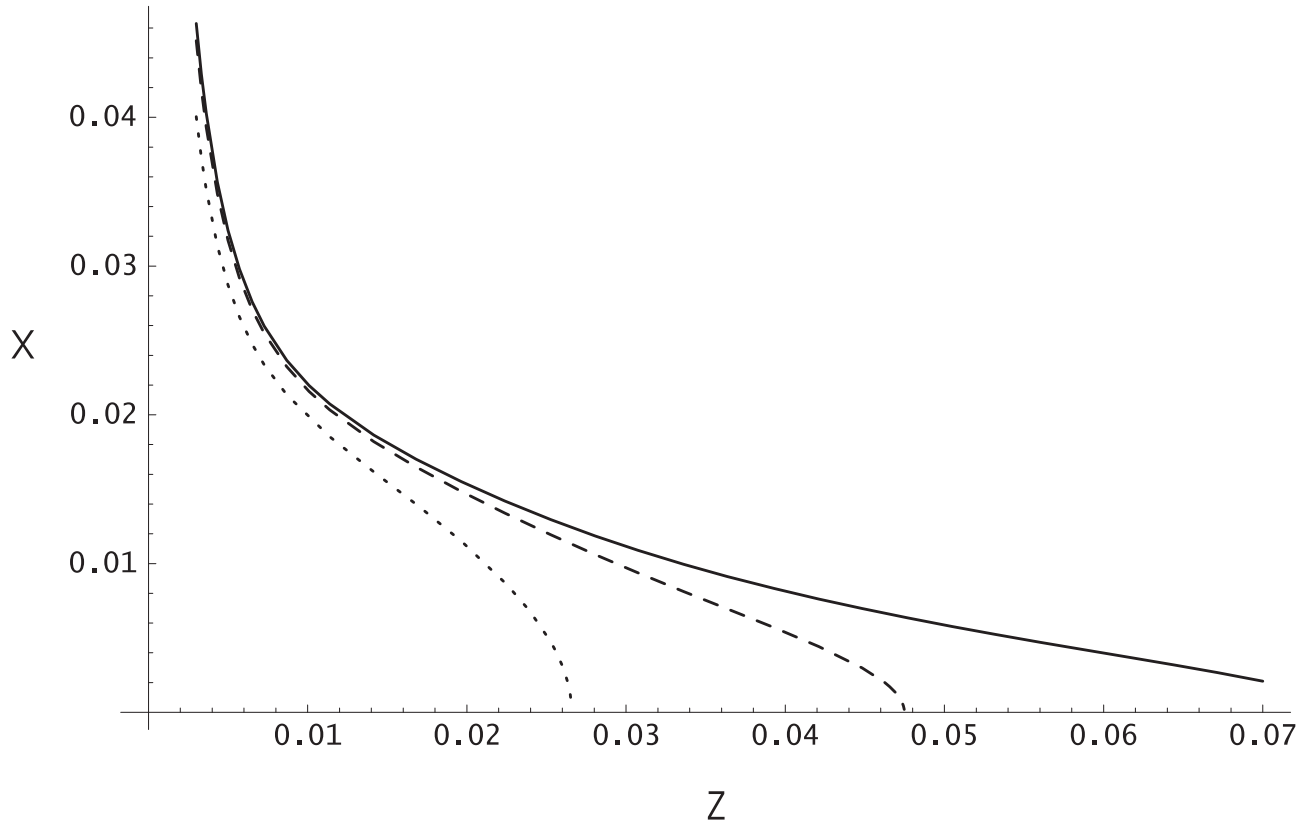

Fig. 1. Resonance diagram of the decay instability: resonant perpendicular wavenumber $X = k_x\lambda_D$ vs. parallel wavenumbers $Z = k_z\lambda_D$ of the resonant Langmuir waves. Parameter $b = \Omega_e/\omega_{pe} = 1.04$ (solid line); 1.1 (dash line), and 1.4 (dot line). The electron thermal velocity $V_{Te}/c = 1/70$.

Using here (36) for $\bar{N}_W$ and (38) for $\bar{N}^*_A$, we get an explicit expression for the nonlinear growth rate:

$$\frac{\gamma^2_{NL}}{\Omega_p^2} = \frac{1}{4}\frac{m_p^2}{m_e^2}\frac{1}{2z\,(z-b)^2+b}\frac{1}{b^2 z}\frac{X^2}{Y^2}\left(\frac{z}{b\,(1+\mu_T)}\frac{\omega_A}{\Omega_p} - Y^2\right)\left(X^2 - s_A\frac{m_e}{m_p}b^3\frac{V_{Te}}{V_A}\frac{b^2-z^2}{z^3}KZ\right)W_L. \tag{45}$$

We use here the pump wave energy normalized to the electron thermal energy:

$$W_L = \frac{k_L^2\,|\varphi_L|^2}{4\pi n_0 T_e} = \frac{|E_L|^2}{4\pi n_0 T_e}.$$

From expression (45) we deduce that the instability of the pump Langmuir wave with $Z = k_{Lz}\lambda_D < 0.02$ critically depends on the propagation direction of the daughter KAWs. For forward propagating KAW, $s_A = 1$, the s_A-dependent term in the second line tends to cancel the instability, and only a weak instability is possible. For $\mu_s \approx 0$, i.e., with classic Alfvén waves (Chian et al. 1994), an even weaker instability exists, which cannot be reproduced by (45) because we ignored corresponding small terms.

For both forward and backward propagating KAWs, $s_A = -1$, the decay rate strongly depends on the perpendicular KAW wavenumber X. It vanishes when X tends to 0 but becomes large when X is increased. A strong instability can develop for sufficiently high values of X.

The nonlinear growth rate may be written in non-dimensional form, useful for analysis:

$$\frac{\gamma_{NL}}{\Omega_p} = G = \sqrt{\frac{1}{4}M^2\frac{BC}{b^2\left(2z\,(z-b)^2+b\right)z}W_L}, \tag{46}$$

where

$$B = \frac{X^2}{Y^2}\left(\frac{z}{b\,(1+\mu_T)}f - Y^2\right); \quad C = X^2 - s_A\frac{b^3}{M}\frac{V_{Te}}{V_A}\frac{b^2-z^2}{z^3}KZ.$$

Here $f = \omega_A/\Omega_p$, $M = m_p/m_e$, and the sign of k_{Az} is given by $s_A = k_{Az}/|k_{Az}|$. For $s_A = \pm 1$, the process becomes strong with growing X. In spite of the relative simple form of the nonlinear growth rate (45)–(46), the situation is complicated by the selectivity of the process: X has to satisfy the resonant relation (39). The dependence of the nonlinear growth rate (46) on the wavenumbers of the Langmuir waves is found numerically for typical coronal parameters in the next section.

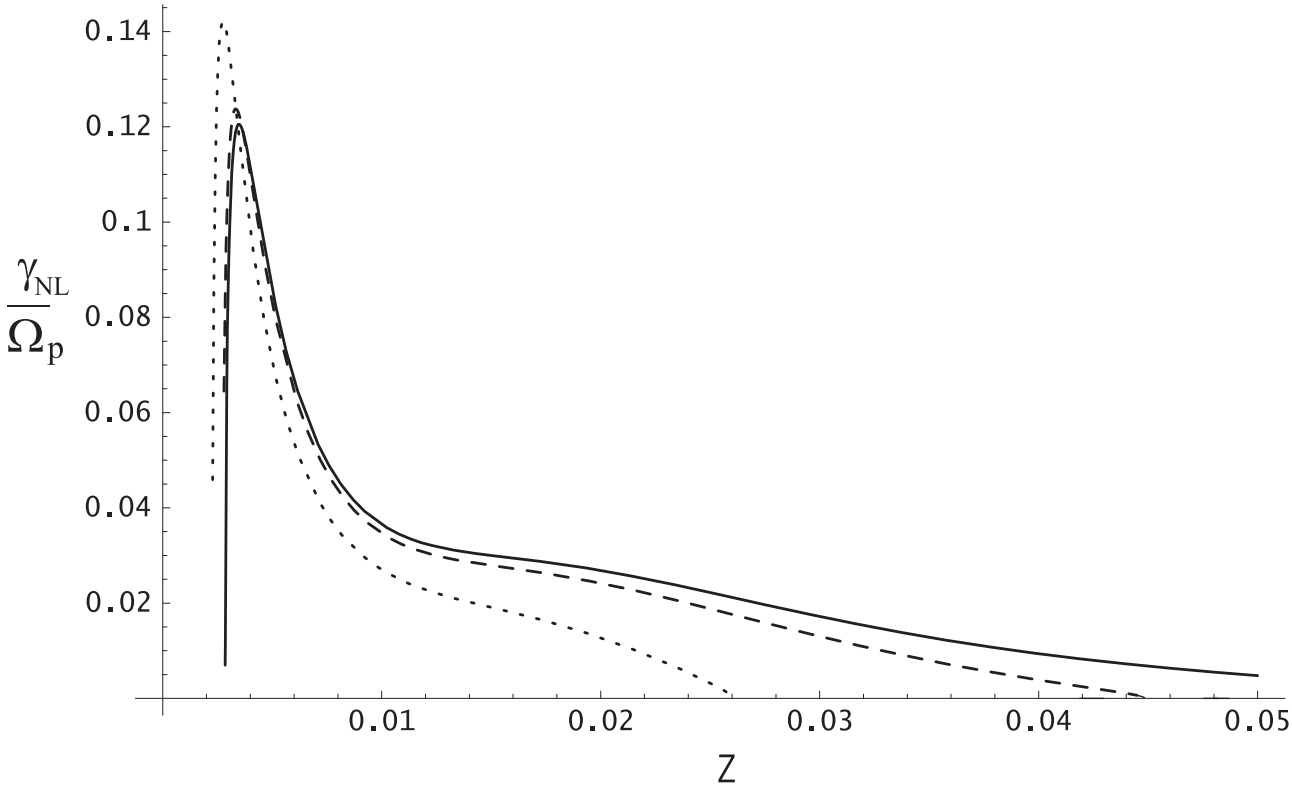

Fig. 2. Nonlinear growth rate of the decay L⇄ KAW + W for Langmuir waves excited in the solar corona by electron beams. For the beam-driven Langmuir waves, the values of the dispersive variable $Z = k_{Lz}\lambda_D = 0.01{-}0.04$ are taken for the spectrum of waves excited by the electron beams with respective velocities $V_b/c = 1/3{-}1/4$. The normalized Langmuir wave energy is $W_L = 10^{-4}$. Parameter $b = \Omega_e/\omega_{pe} = 1.04$ (solid line); 1.1 (dash line), and 1.4 (dot line). The electron thermal velocity $V_{Te}/c = 1/70$.

5. Excitation of the LAW events by electron beams in the solar corona

Electron beams exist in many space and astrophysical plasmas and are identified by remote radio observations and in situ by several satellites; A few examples are the beams related to solar bursts, Earth's foreshocks and Earth's magnetosphere. Langmuir waves are commonly believed to be excited in the solar corona and solar wind by fast electron beams with a relative number density $n_b/n_0 = 10^{-6}{-}10^{-4}$, that are accelerated in coronal magnetic reconnection events to a velocity $V_b \sim (0.1{-}0.5)\,c$. In turn, the beam-driven Langmuir waves produce type III solar radio bursts (Goldman 1983; Melrose 1984). The in-situ satellite observations in the solar wind strongly support the picture that the Langmuir waves are indeed excited by electron beams and eventually lead to solar type III bursts (Dulk et al. 1998; Ergun et al. 1998; Thejappa & MacDowall 1998, and references therein). Other types of waves can be excited by two-dimensional (in velocity space) electron beams, like oblique whistlers, ion-cyclotron and lower-hybrid waves (Zhang et al. 1993; Wong & Smith 1994; Ergun et al. 1998). In this context we note that the bump-on-tail instabilities of the above mentioned modes are far weaker than the Langmuir instability for fast diluted electron beams under coronal/solar wind conditions. As suggested theoretically and observationally, they can only play a complimentary role while the Langmuir instability extracts the main part of the beam energy. Consequently, the observed Langmuir waves are much more intense.

5.1. Parameters

In this paper we focus on the high coronal levels, where the plasma is diluted along the magnetic filaments connected to the cool patches at the coronal base. For example, in the region where the magnetic field $B_0 = 3.5$ G, number density $n_0 = 10^6$ cm^{-3}, and temperature $T_p \approx T_e \approx 10^6$ K, we have the following values for the key parameters of the background plasma: $\Omega_e = 6.2\times10^7$ rad s^{-1}, $\omega_{pe} = 5.6\times10^7$ rad s^{-1} (that is $\Omega_e/\omega_{pe} = 1.09$), $V_A = 7.6\times10^8$ cm/s, $V_{Te} = 3\times10^8$ cm/s (that is $V_A/V_{Te} \approx 3$, $V_{Te}/c \gtrsim 10^{-2}$, $\rho_p \approx 200$ cm).

Typical velocities of electron beams in the solar corona can be deduced from radio observations and from in-situ observations in the solar wind. They lie in the range $V_b \sim (0.1 \div 0.5)\,c$. The initial parallel propagating Langmuir waves that are excited by these beams have parallel wavenumbers $k_{Lz}\lambda_D = V_{Te}/V_b = 0.01 \div 0.05$ for the electron thermal velocity in corona $V_{Te} = 3\times10^8$ cm/s ($T_e \lesssim 10^6$ K). When interplanetary data are extrapolated into the corona (see Cairns & Robinson 1998) we infer the Langmuir wave energy $W_L \lesssim 10^{-4}$.

For any given V_b, the beam-driven Langmuir waves can be in 3-wave resonance with whistlers and KAWs in the regions where the perpendicular wavenumber attains values determined by the resonant condition (39). The initial beam-driven Langmuir waves can excite resonant whistlers and KAWs in the coronal regions where the condition $b = \Omega_e/\omega_{pe} > 1$ is fulfilled. The parameter b can be close to 1, $b \gtrsim 1$, or b can deviate from 1 significantly. The condition $b > 1$ may be satisfied in underdense magnetic filaments at high coronal levels, or in strongly magnetized plasmas in the low corona, where the magnetic field is concentrated in magnetic flux tubes.

5.2. Decay of Langmuir waves driven by fast electron beams

Let us consider the decay instability L $\rightleftarrows$ W + KAW of weakly dispersive Langmuir waves, $Z < Z_1$, which are excited by fast electron beams, $V_b/c \gtrsim 0.3c$. These waves undergo resonant decay in the regions where X attains a value given by resonance condition (40). As it follows from (45), the coupling of Langmuir wave energy into KAWs and parallel whistlers becomes strong for large perpendicular Langmuir/KAW wavenumbers ($k_{Ax} = k_{Lx}$). The frequencies of the excited KAWs are determined by the parallel wavenumber $Z = k_{Lz}\lambda_D$ of the driving Langmuir wave and are given by the frequency matching conditions. Note, however, that the dependence of the nonlinear increment on the KAW frequency is weak, so we set $f = 0.5$. The particular value of the KAWs' frequency is determined from the resonant condition (39) with given Z and X.

The nonlinear growth rate for plasma and Langmuir wave parameters expected in the solar corona is shown in Fig. 2 for antiparallel propagating KAWs ($s_A = -1$). The decay into parallel-propagating KAWs is much weaker for $k_{Lz}\lambda_D < 0.02$, and it is still weaker (but of the same order) for $k_{Lz}\lambda_D \geq 0.02$.

For all values of $b = 1.04$, 1.1 and 1.4, the decay becomes strong for the corresponding resonant perpendicular wavenumbers $X_{res} = 0.02 - 0.04$ (i.e., $k_{Ax}\rho_p \sim 1$). Therefore, the decay condition is $k_{Lx}\lambda_D \approx k_{Lx}^{res}\lambda_D \equiv X_{res}$, and all Langmuir waves that develop these resonant perpendicular wavenumbers, nonlinearly excite resonant whistlers and KAWs.

Langmuir waves can easily develop large perpendicular wavenumbers due to phase mixing in a plasma that is inhomogeneous in the perpendicular (x) direction. When we take $L_x = 10^6$ m for the inhomogeneity length-scale (Woo 1996), and use the evolutionary (Hamilton) equation for k_{Lx} in the form

$$k_{Lx}\lambda_D = \lambda_D \left|\frac{\partial \omega_{pe}}{\partial x}\right| t \approx \frac{\lambda_D}{2L_x}\omega_{pe}t = \frac{V_{Te}}{2L_x}t,$$

we see that the resonant perpendicular wavenumbers, $k_{Lx}\lambda_D \sim 0.02$, are already generated after a very short time of the order 10^{-2} s. Therefore, even if the initial beam-driven Langmuir waves are parallel-propagating, and thus nonlinearly stable, they quickly become oblique and nonlinearly unstable. As follows from (45), the coupling of Langmuir wave energy into KAWs and parallel whistlers becomes strong for these values of perpendicular Langmuir/KAW wavenumbers. The process is thus turned on when a fast electron beam with a given value of velocity $V_b/c \gtrsim 0.3$ passes through the region with the values of $b = 1.04{-}1.4$ and excited by beam Langmuir waves develop perpendicular wavenumbers $k_{Lx}\lambda_D \sim 0.02$. Moreover, Langmuir waves, excited by electron beams in a $b > 1$ plasma, are already oblique (see Discussion), which facilitate the LAW decay instability.

The LAW decay is sensitive to the Langmuir parallel wavenumbers, and its growth rate attains a maximum $\gamma_{NL} \gtrsim 0.1\Omega_i\sqrt{10^4 W_L}$ at $k_{Lz}\lambda_D \sim 0.005$. The wavenumbers of the Langmuir waves excited by fast electron beams are initially about four times bigger, $k_{Lz}\lambda_D \sim 0.02$. For these wavenumbers the growth rate is $\gamma_{NL} \sim 0.025\Omega_i\sqrt{10^4 W_L}$ if Ω_e/ω_{pe} is sufficiently close to unity, $\Omega_e/\omega_{pe} \gtrsim 1$, and the growth rate is highly reduced for larger values of Ω_e/ω_{pe} (see Fig. 2). Thus, the Langmuir waves directly driven by the beams decay strongest in the regions where $\Omega_e/\omega_{pe} \gtrsim 1$.

However, even in regions where Ω_e/ω_{pe} deviates significantly from 1, the Langmuir waves decay fast when they reduce parallel wavenumbers to $k_{Lz}\lambda_D \sim 0.005$. A most probable mechanism reducing parallel Langmuir wavenumber in the solar corona is the density variation along magnetic field lines. So, a local density increase of only

$$\frac{\delta n_e}{n_0} = \frac{15}{16}\left(k_{Lz}^{in}\lambda_D\right)^2 \sim 4\times 10^{-4}$$

could reduce initial $k_{Lz}^{in}\lambda_D = 0.02$ to $k_{Lz}\lambda_D = 0.005$:

$$k_{Lz}\lambda_D = \sqrt{\left(k_{Lz}^{in}\lambda_D\right)^2 - \frac{\delta n_e}{n_0}} = \frac{1}{4}k_{Lz}^{in}\lambda_D \sim 0.005.$$

Although the density on average decreases with heliocentric distance, it can increase locally due to, e.g., presence of low-frequency waves. For example, in the presence of phase-mixed Alfvén waves with wavenumbers $k_z \ll k_{Lz}$, $k_\perp\delta_p = 0.1$, and amplitude $\delta B/B_0 = 0.01$, launched from the coronal base, we expect number density perturbations

$$\left|\frac{\delta n_e}{n_0}\right| = \frac{k_\perp\delta_p}{K}\frac{\delta B}{B_0} \sim 10^{-3},$$

which suffice for shifting the parallel Langmuir wavenumbers in the range of strong decay instability.

Langmuir waves excited by slow beams have also to reduce their $k_{\mathrm{L}z}$ in order to attain the allowed range of parallel wavenumbers specified by (41), or even the range of strong decay instability $k_{\mathrm{L}z}\lambda_{\mathrm{D}} \lesssim 0.01$. Again, this may be done by parallel inhomogeneity: Langmuir waves propagating along B_0 in the direction of increasing number density will decrease their parallel wavenumber. There are also other nonlinear interactions, that tend to reduce the parallel wavenumber of Langmuir waves. In one of these ways all the conditions for the instability can be satisfied even if the Langmuir waves are initially excited with relatively high Z (i.e., by slow beams).

6. Discussion

In the solar wind values of $\Omega_{\mathrm{e}}/\omega_{\mathrm{pe}}$ smaller than 1 are measured in situ, and it is generally accepted that $\Omega_{\mathrm{e}}/\omega_{\mathrm{pe}} < 1$ in the coronal type III bursts. But the coronal heating process is highly non-uniform, which causes large cross-field density variations of the plasma evaporated from chromosphere. As the strong magnetic field (MF) confines the plasma across MF lines, the hydrostatic equilibrium tends to set in along MF lines, which gives rise to a nonuniform plasma density across MF in the high corona. The resulting high plasma pressure variations across MF are easily balanced in a low-β coronal plasma by small variations of the magnetic pressure. These nonuniformities are observed in the form of filamentary ray-like structures of about 1 km width, extending radially from the coronal base in the corona (Woo 1996). The condition $\Omega_{\mathrm{e}}/\omega_{\mathrm{pe}} > 1$ can be satisfied along the low-density magnetic filaments rooted in the underheated parts of the coronal base.

An alternative model to the conventional plasma-emission has been proposed recently by Wu et al. (2002) for coronal type III radio bursts. They suggested that *x*- and *o*-mode electromagnetic waves are directly excited near the electron cyclotron frequency by the electron-cyclotron maser instability (this process is similar to the generation of AKR – auroral kilometric radiation in the Earth's magnetosphere). An essential ingredient of this model is the presence of underdense magnetic fibers with $\Omega_{\mathrm{e}}/\omega_{\mathrm{pe}} > 1$, attributed by Wu et al. to the strong magnetic fields/low-density plasma at the coronal base. Another critical assumption is an intense pitch-angle scattering of beam electrons, possibly due to Alfvén waves. The resulting electron beam distributions can be unstable with respect to Cherenkov (bump-on-tail) and electron-cyclotron instabilities simultaneously. But the parallel electrostatic (i.e., Langmuir-type) instability is still dominant in most cases, as long as the bump-on-tail is present (see, e.g., Zhang et al. 1993). Vlahos & Rowland (1984) studied electron beams under similar conditions and pointed out mechanisms that suppress the pitch-angle scattering, in which case the bump-on-tail Langmuir wave instability is by far dominant.

The (random phase) "electrostatic" decay $\mathrm{L} \rightleftarrows \mathrm{L}' + \mathrm{S}$ into a secondary Langmuir wave and an ion-acoustic wave (or quasi-mode at $T_{\mathrm{e}} \sim T_{\mathrm{p}}$) has been suggested as an efficient nonlinear process for beam-driven Langmuir waves (Cairns & Robinson 1998; Cairns 2000). However, the conclusion about the dominant role of the ion-acoustic mode is not final untill the role of other wave modes is investigated sufficiently. In particular, the kinetic Alfvén mode can participate in Langmuir decay, giving rise to a low-frequency electromagnetic decay $\mathrm{L} \rightleftarrows \mathrm{L}' + \mathrm{KAW}$ and/or modulational instability (Voitenko et al., in preparation).

In the present paper we have dealt with another new nonlinear process in which kinetic Alfvén waves participate: the parametric excitation of KAWs and whistler waves by Langmuir waves. The interest in this process is stimulated by the radio observations of complex wave events in the solar corona where Langmuir waves are supposed to be excited by electron beams. Our study suggests that the Alfvén-whistler turbulence may provide an efficient energy sink for Langmuir waves in a diluted solar plasma where the local electron-cyclotron frequency is higher than the local plasma frequency.

Let us compare the growth rates of the competing parametric decays $L \rightleftarrows \mathrm{W} + \mathrm{KAW}$ and $\mathrm{L} \rightleftarrows \mathrm{L}' + \mathrm{S}$, keeping in mind that the condition $\Omega_{\mathrm{e}}/\omega_{\mathrm{pe}} > 1$ is required for the decay into whistlers. The process $\mathrm{L} \rightleftarrows \mathrm{L}' + \mathrm{S}$ is well studied for $\Omega_{\mathrm{e}}/\omega_{\mathrm{pe}} < 1$, typical in the solar wind (see, e.g., Cairns & Robinson 1998, and references therein). However, there are much fewer studies of the electrostatic decay in a low-density/strong magnetic field regime $\Omega_{\mathrm{e}}/\omega_{\mathrm{pe}} > 1$, which is sometimes called supercritical (Newman et al. 1994a). In comparison to the subcritical ($\Omega_{\mathrm{e}}/\omega_{\mathrm{pe}} < 1$) regime, there are two modifications: the perpendicular dispersion of Langmuir waves can change its sign (see Eq. (23)), and the electrostatic decay is primarily into oblique Langmuir and ion-acoustic waves (Newman et al. 1994a,b; Akimoto 1995).

As a strong temperature anisotropy $T_{\mathrm{e}}/T_{\mathrm{p}} = 4{-}5$ has been assumed in these studies, direct comparison of our LAW growth rate with the growth rate of the oblique electrostatic decay (L-oL) calculated by Newman et al. and by Akimoto is impossible. If we formally compare the LAW growth rate $\gamma_{NL}\,(\mathrm{LAW}) \sim 0.1\Omega_{\mathrm{p}}\sqrt{10^4 W_{\mathrm{L}}}$ (valid for $Z \sim 0.01$, $T_{\mathrm{e}}/T_{\mathrm{p}} \sim 1$) with the L-oL growth rate given by Akimoto (1995) $\gamma_{NL}\,(\mathrm{LoL}) \sim 0.1\omega_{\mathrm{pp}}\sqrt{10 W_{\mathrm{L}}}$ (valid for $T_{\mathrm{e}}/T_{\mathrm{p}} \sim 5$, where the ion sound damping $\gamma_{\mathrm{s}}/\omega_{\mathrm{s}} \ll 1$), we obtain $\gamma_{NL}\,(\mathrm{LAW})\,/\gamma_{NL}\,(\mathrm{LoL}) \sim \Omega_{\mathrm{e}}/\omega_{\mathrm{pe}}$, i.e., $\gamma_{NL}\,(\mathrm{LAW})$ and $\gamma_{NL}\,(\mathrm{LoL})$ are of the same order for $\Omega_{\mathrm{e}}/\omega_{\mathrm{pe}} \sim 1$. For higher Langmuir wavenumbers, $Z \gtrsim 0.02$, $\gamma_{NL}\,(\mathrm{LoL}) > \gamma_{NL}\,(\mathrm{LAW})$. However, the ion-acoustic wave is heavily damped for coronal temperatures where $T_{\mathrm{e}}/T_{\mathrm{p}} \sim 1$, and the growth rate of the electrostatic decay can fall below $\gamma_{NL}\,(\mathrm{LAW})$. In our opinion, the process $\mathrm{L} \rightleftarrows \mathrm{W} + \mathrm{KAW}$ competes with the electrostatic decay in isothermal plasmas, $T_{\mathrm{e}} \sim T_{\mathrm{p}}$, where the efficiency of the electrostatic decay is reduced by the strong damping of ion-acoustic mode. These estimations indicate that an additional study is required to determine what process is stronger for particular values of $T_{\mathrm{e}}/T_{\mathrm{p}}$ and Z.

The monochromatic parametric description that we used is justified when the nonlinear growth rate exceeds the bandwidth of the decaying waves. This approach has been extensively used for the narrow-band Langmuir waves (see Bárta & Karlický 2000, and references therein). The bandwidth of the Langmuir waves excited by electron beam is proportional to the beam velocity spread. Let us consider a simple case when the Langmuir bandwidth is determined by the parallel wave dispersion (23) with

($X = 0$). The energy of excited Langmuir waves is concentrated slightly above the wavenumber determined from the resonant condition,

$$Z_{\min} = \frac{V_{Te}}{V_b}.$$

The upper boundary of the spectrum $Z_{\max}$ may be estimated from the velocity spread of beam ΔV_b:

$$Z_{\max} = \frac{V_{Te}}{V_b - \Delta V_b},$$

and, for $\Delta V_b / V_b \ll 1$, the bandwidth is

$$\omega_L(Z_{\max}) - \omega_L(Z_{\min}) \approx \omega_{pe} Z_{\min}^2 \frac{\Delta V_b}{V_b}.$$

The parametric approach that we use is justified if

$$\frac{\gamma_{NL}}{\Omega_p} > \frac{\omega_L(Z_{\max}) - \omega_L(Z_{\min})}{\Omega_p} \approx \frac{m_i}{m_e} Z_{\min}^2 \frac{\Delta V_b}{V_b}.$$

This condition can be satisfied for high-energy narrow beams in the cool filaments in the solar corona ($Z_{\min} \sim 0.01$, $\Delta V_b / V_b < 0.3$).

Otherwise, when the nonlinear growth rate is less than the bandwidth of the decaying waves, the random phase version of decay should be considered (Cairns & Robinson 1998). We plan to do this in our future studies. Obviously, the decay growth rate in this case is reduced by the decoherence of waves.

The bandwidth of secondary waves depends on how broad maximum has the growth rate as a function of wavenumbers of these secondary waves. Even in the case of monochromatic pump, a broadband spectrum of secondary waves can be excited if the growth rate is relatively flat. Of course, this spectrum still consists of wave pairs, each being in the three-wave parametric resonance with the pump wave.

As for the question how to distinguish between the modes of interest (i.e., KAWs and whistlers) excited by Langmuir waves, and the modes driven directly by beams. It is important for the identification of dominant processes and remote diagnostics. To this end we note that the fast $0.3c$ electron beam cannot generate KAWs directly via bump-on-tail instability. Indeed, the KAW dispersion (14) restricts the wave phase velocity to the range $\min\{V_A; (1 + T_i/T_e) V_{Te}\} < \omega_A / k_{Az} < \max\{V_A; (1 + T_i/T_e) V_{Te}\}$, and since both V_A and $(1 + T_i/T_e) V_{Te}$ are much smaller than the beam velocity ($V_b \sim 0.3c$), the KAWs are off-resonant with the beam, and, consequently, cannot extract energy from it. Even if the Alfvén waves driven by an alternative source are present (see, e.g., Verheest 1990), we believe that the formulae we provide here are sufficient to distinguish the Langmuir-driven KAWs. In particular, cross-field KAW wavelengths, determined from the resonant conditions, in turn determine the scales and velocities of the electron density perturbations (30) associated with KAWs. In terms of KAW magnetic field perturbations $\delta B_A / B_0$, the relative density perturbations are

$$\left| \frac{\delta n_e}{n_0} \right| = \frac{k_{A\perp} \delta_p}{K} \frac{\delta B_A}{B_0}.$$

Since the decay involving sunward propagating KAWs ($s_A = -1$) is stronger, the corresponding sunward moving density perturbation could be well distinguished from the perturbation produced by waves propagating from the Sun. As far as whistlers is concerned, we point out a striking difference: the Langmuir-driven whistlers are strongly correlated with Langmuir waves, whereas the beam-driven whistlers and Langmuir waves tend to be anti-correlated (e.g., Ergun et al. 1998). The observations support a hypothesis that the whistlers in solar wind are excited mainly by beams, so that the process $L \rightleftarrows KAW + W$ is not occurring. It is not surprising, because $\Omega_e / \omega_{pe} < 1$ in the solar wind beyond 0.3 AU, where three-wave resonance is impossible. However, these observations do not exclude that process in the solar corona where the condition $\Omega_e / \omega_{pe} > 1$ can be satisfied.

As the LAW decay exhibits a strong dependence on the pump Langmuir wavenumbers, and the electrostatic decay is relatively insensitive, the interplay between these two nonlinear processes can be complicated. For example, the beam-driven parallel Langmuir waves could first undergo electrostatic decay processes redistributing their energy towards resonance perpendicular wavenumbers, and then LAW decays come into play and eventually supplies a sink for Langmuir turbulence.

The nonlinear process that we have discussed here may play a role also in the auroral zone of the Earth's magnetosphere, where LAW events are registered in-situ by satellites. Spacecrafts frequently measure intense bursts of LAW events in conjunction with field-aligned electrons in the auroral zones (Chian et al. 1994). It is interesting to note that despite of significant perpendicular inhomogeneities, the observed Langmuir waves' propagation is confined to within 10° of the geomagnetic field in the auroral zone (Newman et al. 1994a,b). This means that oblique wave propagation is suppressed, which can be accounted for by the dispersion and damping of oblique Langmuir waves (Newman 1994a). At the same time, this effect may be due to the process that we study here: a strong decay of Langmuir waves into whistlers and KAWs when the Langmuir waves develop resonant

perpendicular wavenumbers. For example, for $\Omega_e/\omega_{pe} = 1.1$ and $k_{Lz}\lambda_{De} = 0.025$, the nonlinear Langmuir decay into KAWs and whistlers occurs at the propagation angle θ_{res} ($\tan\theta_{res} = k_{res}/k_{Lz}$) about 11°.

As far as the dynamics of electron beams is concerned, the situation in auroral zones is complicated by the high beam density $n_b/n_0 \gtrsim 10^{-2}$. This introduces dispersive effects, and strong pitch-angle scattering of downward electrons accelerated by electric field. The resulting electron beam distributions become unstable with respect to electron-cyclotron instability and generate AKR emission, but the Cherenkov (bump-on-tail) Langmuir instability is dominant in most cases when the bump-on-tail is present (Zhang et al. 1993).

7. Conclusions

We have investigated a new nonlinear process that is caused by kinetic properties of oblique (kinetic) Alfvén waves: parametric decay L $\rightleftarrows$ W + KAW. This is plausible for the backward propagating KAWs. The nonlinear growth rate strongly increases with growing perpendicular wavenumber, or μ_s – dispersion variable of the KAW. Weakly dispersive Langmuir waves, excited by fast electron beams with $V_b \gtrsim 0.3c$, decay fastest.

We have applied our results to the beam-driven Langmuir waves in the solar corona and found a very short characteristic time scale for the instability to develop, $\tau \sim \gamma_{NL}^{-1} \sim 10^{-4}$ s for the parameters of coronal Langmuir waves deduced from observations. As the nonlinear coupling of Langmuir energy into whistlers and KAWs is possible if $\Omega_e/\omega_{pe} > 1$, the formation of the LAW turbulence is expected in the regions of solar corona where the magnetic field is strong and/or the plasma is dilute. The condition $\Omega_e/\omega_{pe} > 1$ can be satisfied in the thin (~10 km) underdense filaments guided by the magnetic field lines which are connected to the low-temperature patches at the coronal base.

The growth rate of LAW decay critically depends on the parameter Ω_e/ω_{pe} in the range $k_{Lz}\lambda_D \gtrsim 0.01$: it is large for $\Omega_e/\omega_{pe} \gtrsim 1$, but quickly decreases with increasing Ω_e/ω_{pe}. So, the general tendency is that the faster electron beams in $\Omega_e/\omega_{pe} \gtrsim 1$ regions are most efficient for producing of LAW events. The decay instability can develop if $k_{Lx} \gtrsim k_{res}$, where k_{res} is the resonant perpendicular wavenumber that depends on the particular parallel wavenumber of the Langmuir wave (Eq. (40)). Since for typical coronal parameters the resonant perpendicular wavenumber is less than the parallel wavenumber, $k_{res} < k_{Lz}$, the propagation of the non-decaying Langmuir waves is restricted to the cone $\tan\theta = k_{Lx}/k_{Lz} < k_{res}/k_{Lz} < 1$, i.e., to the quasi-parallel propagation.

The situation can be different when local density variations along magnetic field lines are present. These may be produced by, e.g., phase-mixed Alfvén waves, launched from the coronal base. In this case the Langmuir waves, propagating against the density gradient, can reduce their parallel wavenumbers to the range $k_{Lz}\lambda_D \lesssim 0.01$, where the decay instability is very strong and less sensitive to Ω_e/ω_{pe}.

The presence of KAWs in the underdense filaments results in fluctuations of the plasma density and velocity at length-scales 10−100 m across the magnetic field and 1−10 km along the magnetic field. As the instability is much stronger for antiparallel (i.e., sunward) propagating KAWs ($s_A = -1$), the density perturbations produced by Langmuir-driven KAWs should move sunward. Such fluctuations, moving with the Alfvén velocity along the filaments towards the Sun, should give rise to the scattering and/or thin structures of the coronal radio emission. In addition, the traces of these scattering filaments from the distant corona down to the active regions have to pinpoint the places where the plasma is dilute and the electron beams are accelerated.

All these features can be used for diagnostic purposes, and analysis of radio data can provide observational pros and cons of the actual importance of LAW events excited by electron beams in the solar corona.

Acknowledgements. This publication results from the collaborative research in the framework of WISER – World Institute for Space Environment Research (`www.cea.inpe.br/wiser`). Yu. Voitenko acknowledges the financial support by the FWO Vlaanderen (grants G.0335.98 and G.0178.3), and by the Onderzoeksfonds of the K.U. Leuven (project OT/02/57). O. Sirenko acknowledges the financial support by the K.U. Leuven (grant DB.OO.18) and by the FWO Vlaanderen (grant G.0178.3). A. C.-L. Chian acknowledges the award of an 1A Senior Research Fellowship by CNPq. The authors would like to thank the referee for his valuable comments and suggestions that helped us to improve our paper.

References

Akimoto, K. 1995, Phys. Plasmas, 2, 649
Bárta, M., & Karlický, M. 2000, A&A, 353, 757
Cairns, I. H. 2000, Phys. Plasmas, 7, 4901
Cairns, I. H., & Robinson, P. A. 1998, ApJ, 509, 471
Chen, L. 1977, Plasma Phys., 19, 47
Chian, A. C.-L., Lopes, S. R., & Alves, M. V. 1994, A&A, 290, L13
Chian, A. C.-L., Abalde, J. R., Alves, M. V., & Lopes, S. R. 1997, Sol. Phys., 173, 199
Chian, A. C.-L., & Abalde, J. R. 1999, Sol. Phys., 184, 403
Chian, A. C.-L., Borotto F. A., Lopes, S. R., & Abalde, J. R. 2000, Planet. Space Sci., 48, 9
Chian, A. C.-L., Borotto F. A., & Rempel E. L. 2002, Nonlinear Proc. Geophys., 9, 1

Dulk, G. A., Leblanc, Y., Robinson, P. A., Bougeret, J.-L., & Lin, R. P. 1998, J. Geophys. Res., 103, 17223
Ergun, R. E., Larson, D., Lin, R. P., et al. 1998, ApJ, 503, 435
Ginzburg, V. L., & Zhelezniakov, V. V. 1958, Soviet Astron., 2, 653
Goldman, M. V. 1983, Sol. Phys., 89, 403
Grognard, R. J.-M. 1982, Sol. Phys., 81, 173
Hollweg, J. V. 1999, J. Geophys. Res., 76, 14811
Lopes, S. R., & Chian, A. C.-L. 1996, A&A, 305, 669
Luo Q., Chian, A. C.-L., & Borotto F. A. 1999, A&A, 348, L13
Mel'nik, V. N., Lapshin, V., & Kontar, E. 1999, Sol. Phys., 184, 353
Melrose, D. B. 1985, in Solar Radiophysics, ed. D.J. McLean, & N.R. Labrum (New York: Cambridge Univ. Press), 177
Newman, D. L., Goldman, M. V., Ergun, R. E., & Boehm, M. H. 1994a, J. Geophys. Res., 99, 6367
Newman, D. L., Goldman, M. V., & Ergun, R. E. 1994b, J. Geophys. Res., 99, 6377.
Papadopoulos, K., Goldstein, M. L., & Smith, R. A. 1974, ApJ, 190, 175
Robinson, P. A. 1992, Sol. Phys., 139, 147
Ryutov, D. D., & Sagdeev, R. Z. 1970, Sov. Phys JETP, 31, 396
Taranenko, Iu. N., & Chmyrev, V. M. 1987, Geomagnetizm i Aeronomiia (ISSN 0016-7940), 27, 664 (in Russian)
Thejappa, G., & MacDowall, R. J. 1998, ApJ, 498, 465
Verheest, F. 1990, in Basic plasma processes on the sun, ed. E. R. Priest, & V. Krishan (Dordrecht, The Netherlands: Kluwer), 383
Vlahos, L., & Rowland, H. I. 1984, A&A, 139, 263
Voitenko, Yu. M. 1998, J. Plasma Phys., 60, 497
Voitenko, Yu. M., & Goossens M. 2000, A&A, 357, 1073
Yukhimuk, A. K., Voitenko, Yu. M., Yukhimuk, V. A., & Fedun, V. N. 1998, J. Plasma Phys., 60, 485
Yukhimuk, A. K., Yukhimuk, V. A., Sirenko, O. K., & Voitenko, Yu. M. 1999, J. Plasma Phys., 62, 53
Wong, H. K., & Smith C. W. 1994, J. Geophys. Res., 99, 13,373
Woo R. 1996, Nature, 379, 321
Wu, C. S., Wang, C. B., Yoon, Peter H., Zheng, H. N., & Wang, S. 2002, ApJ, 575, 1094
Zaitsev, V. V., Mityakov, N. A., & Rapoport, V. O. 1972, Sol. Phys., 24, 444
Zakharov, V. E., Musher, S. L., & Rubenchik, A. M. 1985, Phys. Rep., 129, 285
Zhang, Y.L., Matsumoto, H., & Omura, Y. 1993, J. Geophys. Res., 98, 21, 353